Shock Waves
DOI 10.1007/s00193-016-0621-8

ORIGINAL ARTICLE

Characterisation of blast loading in complex, confined geometries using quarter symmetry experimental methods

T. Anthistle[1] · **D. I. Fletcher**[1] · **A. Tyas**[2]

Received: 29 August 2014 / Revised: 28 November 2015 / Accepted: 6 January 2016

Abstract Explosions in confined spaces lead to complicated patterns of shock wave reflection and interactions which are best investigated by use of experimental tests or numerical simulations. This paper describes the design and outcome of a series of experiments using a test cell to measure the pressures experienced when structures were placed inside to alter the propagation of shock waves, utilising quarter symmetry to reduce the size of the required test cell and charge. An 80 g charge of PE4 (a conventional RDX-based plastic explosive) was placed at half height in one corner of the test cell, which represents the centre of a rectangular enclosure when symmetry is taken into consideration. Steel cylinders and rectangular baffles were placed within the test cell at various locations. Good reproducibility was found between repeated tests in three different arrangements, in terms of both the recorded pressure data and the calculated cumulative impulse. The presence of baffles within the test cell made a small difference to the pressures and cumulative impulse experienced compared to tests with no baffles present; however, the number and spacing of baffles was seen to make minimal difference to the experienced pressures and no noticeable difference to the cumulative impulse history. The paper presents useful experimental data that may be used for three-dimensional code validation.

Communicated by C. Needham and G. Ciccarelli.

✉ T. Anthistle
tom.anthistle@gmail.com

D. I. Fletcher
D.I.Fletcher@Sheffield.ac.uk

[1] Department of Mechanical Engineering, University of Sheffield, Mappin Street, Sheffield S1 3JD, UK

[2] Department of Civil and Structural Engineering, University of Sheffield, Mappin Street, Sheffield S1 3JD, UK

Keywords Confined explosion · Shock reflection · Quarter symmetry experiments · Rigid baffles

1 Introduction

The behaviour of shock waves within structures is of interest to engineers in many fields, particularly to those looking at the design of structures that may be subject to an internal explosion. The origin of the current work is the question of whether the internal design of a rail vehicle can beneficially change outcomes for passengers in the event of a terrorist attack, but is framed here in more general terms that are more widely applicable. Particular geometrical features within an enclosure (e.g., a rail vehicle) may act to focus reflected shocks, or shield a particular area from exposure to shock waves. This can have important consequences for both physical structures and any persons present inside. Numerical models are increasingly used to predict the behaviour of shock waves in complex environments as well as the effects that shock waves have on structures within an enclosure using coupled solutions for the structural dynamics and the fluid behaviour. These models are useful where experiments are too costly, complex or time consuming, but it is important that models are validated against experimental data.

The experimental testing presented here was undertaken with a number of aims in mind: first, to generate data for validation of numerical modelling [1]; secondly, to develop an experimental method using quarter symmetry and scaling to reduce the test and charge size needed, increasing the number of configurations which could be tested in a given time and cost; thirdly, to understand the effect of changes in enclosure geometry on measured pressure and impulse; and lastly to generate data showing the consistency of output from high explosive detonations in confined spaces that can pro-

Published online: 02 March 2016

vide the basis for future validations of a variety of prediction tools.

There have been a number of investigations concerning the detonation of high explosives in confined spaces, although very little relates directly to rail vehicles. Work has been done to quantify how tunnels alter the behaviour of shock waves. This includes the effects of branching in tunnels [2], as well as the effects of wall roughness elements [3,4]. Smith et al. [3] used scaled (1:30) experiments to investigate how altering the size and number of roughness elements along a tunnel alters the pressure history. The work concludes that roughness could offer a means of protecting a structure when placed between a sensitive structure and the point of detonation. Work by Neuscamman [5] and Pope [6] indicates that secondary combustion or "afterburn" can be responsible for some of the overpressure experienced in confined tunnels.

Smith et al. used small-scale models of both tunnel networks [3] and cuboidal geometries [7] to demonstrate the applicability of scaling to confined blast loads. Sauvan et al. [8] conducted scaled experiments using a four-wall enclosure and propane–oxygen mixtures, while Togashi et al. [9] conducted experiments and numerical models of a variety of explosive materials in linked rooms to validate numerical modelling of afterburning energy. They found that afterburn changed the pattern of shock reflection and increased the cumulative impulse. Looking more widely than just tunnels, Keenan [10] provided curves for the pressures experienced inside and outside cubicles of different size and number of walls, primarily to aid the design of weapons storage facilities. Wu et al. [11] investigated confined explosions in a full-scale blast chamber, using a variety of charge shapes and positions. Edri et al. [12] carried out experiments on a single room using TNT charges at a variety of masses, identifying some discrepancies between empirical prediction tools and experimental data.

The work presented here aims to extend much of the work above, by introducing symmetry to experimental testing as well as scaling, and varying the geometry to understand how this alters the pressure and cumulative impulse histories.

2 Experimental procedure

2.1 Test cell layouts

A series of three test arrangements were designed, with vertically positioned cylinders and a varying number of disrupting elements or baffles along one wall. Test arrangements are referred to as A1, A2 and A3, which are shown in Fig. 1. Vertical boundary walls in the test cell are referred to as A, B and C, as shown in Fig. 1.

Test arrangement 1 (A1) contained no baffles on wall C, and two vertical cylinders with a height of 814 mm and a diameter of 114 mm placed with their centres 990 and 1980 mm from wall B and 364 mm from wall A. This provided a base case for comparison with other test arrangements to identify the effect of baffles on both the wall on which they are placed (C) and the wall opposite (A). A2 and A3 both have a number of baffles along wall C, which are spaced at 990 mm intervals along the wall in A2 and 745 mm in A3. The baffles were fixed in place with lengths of mild steel angle section and mechanical fasteners, and the cylinders were fastened to the base of the test cell using lengths of M20 threaded rod. The walls and cylinders were intended to behave as rigid bodies.

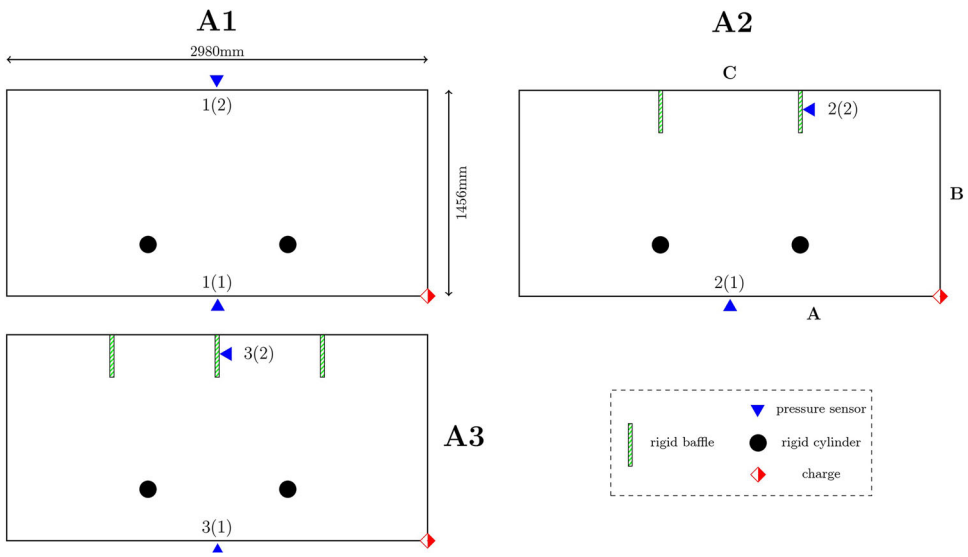

Fig. 1 Plan view of the three test arrangements, including overall dimensions

2.2 Quarter symmetry testing

Walls A and B in Fig. 1b represent an experimental approximation of symmetry planes. Symmetry planes are often used numerically to reduce the size of the models (or increase resolution within the available resources), but are rarely implemented in experimental testing of this type. The walls of the test cell were made of 19 mm mild steel, which for the charge size used ensures that any deflection of the walls are negligible. For symmetric shocks (i.e., two shocks meeting at a symmetry plane), the interaction of the shocks is analogous to reflection [13], in this case the reflection of shocks at the symmetry plane of walls A and B.

To ensure that the initial blast wave travels parallel to the symmetry planes, half-hemispherical charges were used, as shown in Fig. 2, with the flat sides of the charge flush with the symmetry planes, walls A and B. To allow the charge and detonator to be easily assembled, positioned and mounted, the charge was mounted on a metal hinge and secured once the charge and detonator assembly was satisfactory. To ensure that the flat surfaces of the charge were flush with walls A and B of the test cell, and to protect metal on the face of the hinge (particularly, the hole through which the detonator was inserted), a sacrificial standoff packing of layered and bonded corrugated fibreboard was first attached to the hinge using adhesive tape. Once the standoff packing was in place, a detonator was inserted through the hinge corner and a breakwire to trigger data acquisition wrapped around it and fixed in place. An 80 g charge of PE4 (a conventional RDX-based plastic explosive) was moulded using a sintered nylon mould, shown in Fig. 2a, and placed in position with the detonator inserted, as indicated by the hole shown in Fig. 2b. Once the charge and detonator were connected, the charge was fixed in place and the hinge closed and secured, as shown in Fig. 3. Shock tube non-electric detonators were used throughout.

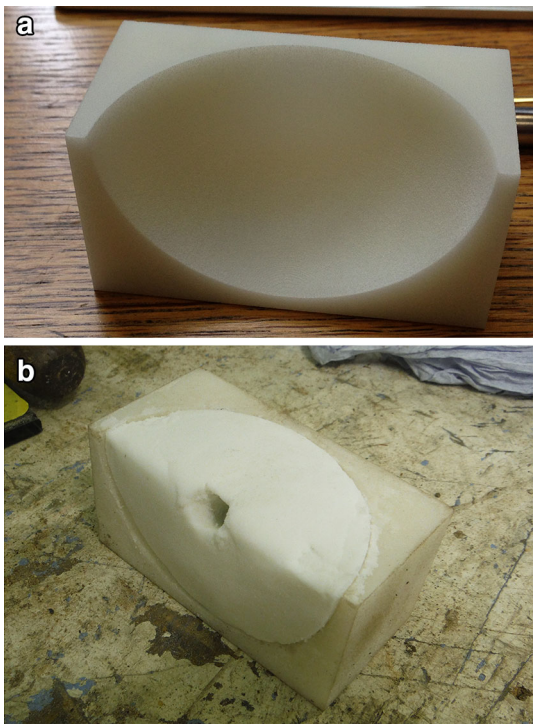

Fig. 2 Moulding of charge

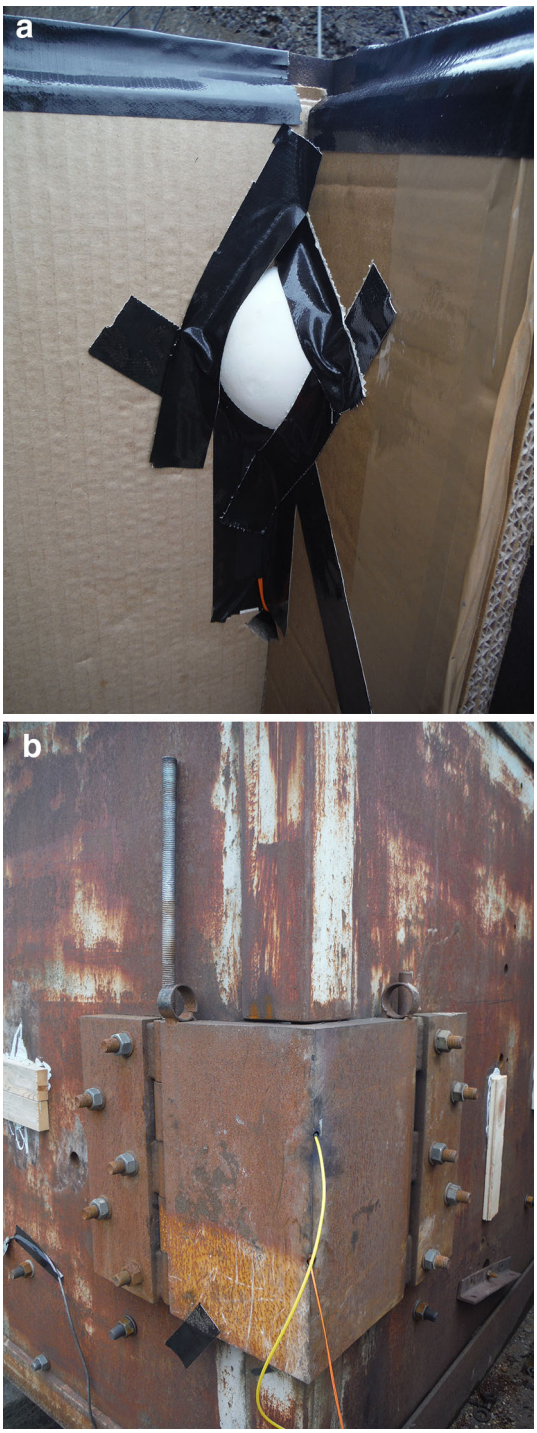

Fig. 3 Positioning of charge

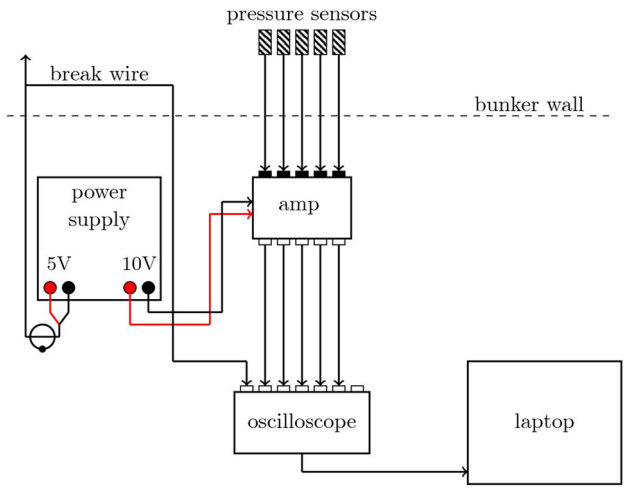

Fig. 4 Data acquisition schematic

Within the test cell, pressures were measured at five locations in each test. This provided some redundancy in the measurements in case of sensor failure, with Fig. 1 showing only the position of sensors from which data were used. With hindsight, a greater number of pressure measurement locations would have helped to build an improved picture of the pressure reflection behaviour, but a limited number of appropriate sensors were available. The locations were also chosen to ensure that pressure sensors were protected from detonator fragmentation and fireball heating effects. Kulite HEM and HKM piezoresistive pressure sensors were used throughout, which were fitted so that they were flush with the inner surface of the test cell. Sensors were attached to charge amplifiers and then via TiePie USB oscilloscopes to a laptop, which recorded data in 14-bit resolution at 1.53 MHz for 55 ms, with a pre-trigger data capture of 6 ms. Data capture was triggered using a powered breakwire wrapped around the detonator. The data acquisition configuration is shown in Fig. 4. Raw pressure history data were filtered using a ninth-order low pass Butterworth filter with a normalized cutoff frequency of 0.02.

3 Pressure and cumulative impulse history

3.1 A1 results

Pressure history and cumulative impulse data for two sensor locations in arrangement 1 are shown in Figs. 5, 6, with the pressure history plotted over the first 20 ms and cumulative impulse plotted over the whole measured time of 55 ms. The pressure and cumulative impulses shown in Fig. 5a, b are from the sensor on wall A and represent the pressures on the symmetry plane. The first thing to note in Fig. 5a is the presence of a high-frequency signal in the data that begins at 0.5 ms and continues up until the first shock arrives at the sensor at 1.6 ms, and is caused by direct transmission

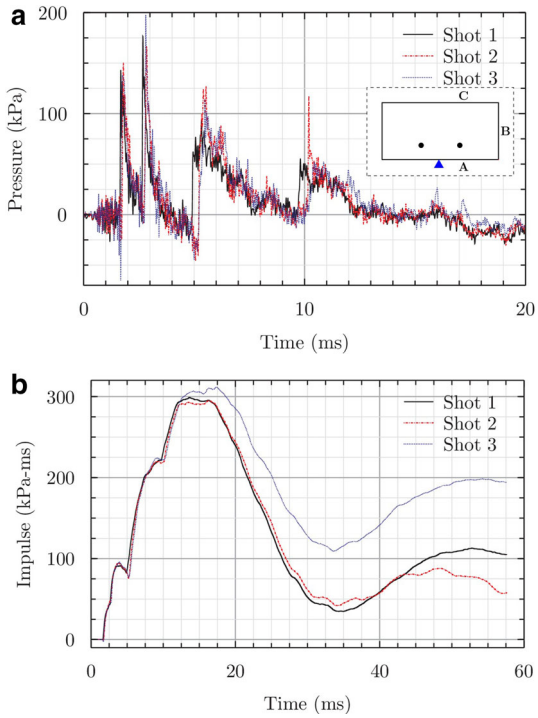

Fig. 5 Data from arrangement 1, location 1

of shock from detonation in the walls of the test cell. This additional signal is only seen when sensors are mounted on walls directly in contact with the charge. The first peak at 1.6 ms represents the side-on overpressure and shows good consistency across all shots with peak values of 140–150 kPa. The consistency in the next three pressure peaks is slightly reduced, with peaks (i.e., shocks) arriving earlier in shot 1 than in others, and some minor discrepancy in peak pressures between shots. Despite this, Fig. 5b shows that over the first 12 ms, where all the significant shock reflection takes place, the cumulative impulse is consistent across all three shots. Cumulative impulse is determined from the integral of pressure over time, so any small differences in pressure history between shots become more visible in cumulative impulse plots. Consequently, where cumulative impulse agrees well between shots, this is a good indication of pressure history similarity.

Data from the pressure sensor on wall C is shown in Fig. 6. The first two pulses in Fig. 6a (indicating the arrival of 2 shocks) show good consistency, albeit with a range of peak pressures for the second pulse between 325 and 380 kPa. The impulse is therefore consistent over the duration of these first two pressure pulses, but from 6 ms pressure peaks generated by shot 1 arrive consistently earlier than from shots 2 or 3. Cumulative impulses over the full 55 ms monitored showed excellent consistency for shots 2 and 3, with diverging cumulative impulse for shot 1 from 6 ms onwards.

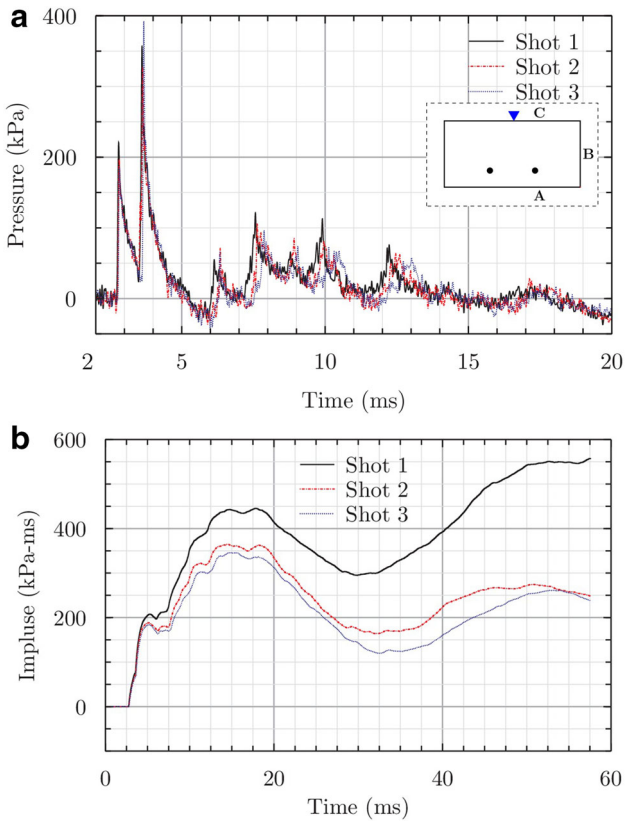

Fig. 6 Data from arrangement 1, location 2

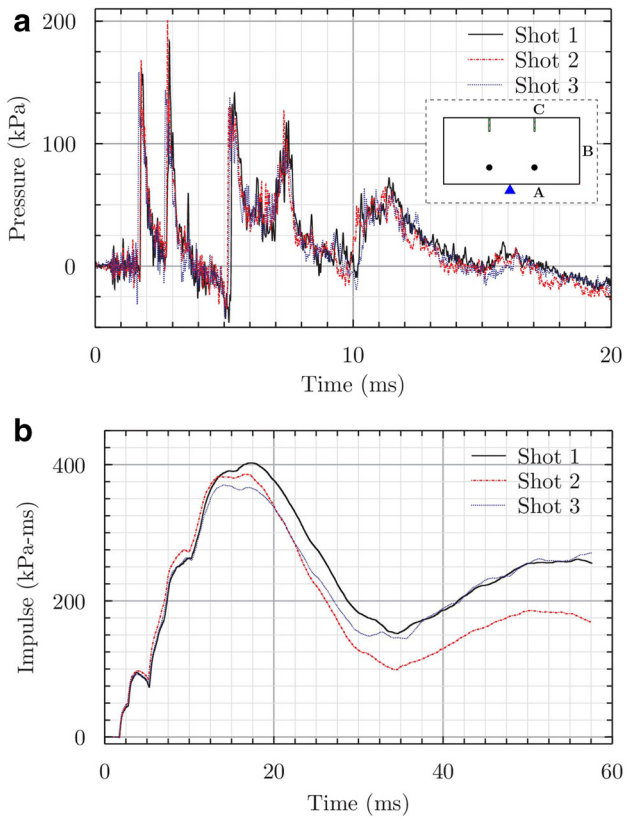

Fig. 7 Data from arrangement 2, location 1

3.2 A2 results

Figure 7a, b shows data from A2, with one sensor in the same place on wall A as in A1, and one placed centrally on the first baffle. The first two pulses in Fig. 7a correspond well with those in the same locations in Fig. 5a, with a similar spread of peak pressures seen in both, but with A1 generally showing slightly lower measured peak values for the first pulse. It is known that this first peak is the side-on pressure, but the similarity between the first and second peaks confirms that the presence of baffles on wall C does not influence the pressures experienced at this location over the first 4 ms. The first reflections from wall C arrive at 5 ms as seen in A1, but are generally of slightly higher magnitude, with a minimum peak value in A1 of 90 kPa, versus a minimum in A2 of 130 kPa. Figure 7a shows a pressure pulse at 8.4 ms, which is not seen in A1, indicating a direct effect from the baffles. Combined with a longer positive overpressure duration in A2 between 10 and 14 ms, this leads to a higher peak cumulative impulse at 17 ms, as shown in Fig. 7b. It is interesting to note that despite the different number and duration of pulses in A1 and A2, the shape of the cumulative impulse curve is almost identical.

Pressures and impulses measured on the face of the baffle in A2 are shown in Fig. 8. A more complex pattern of shock reflection is indicated in Fig. 8a relative to position 1 in the same test arrangement, largely down to the direction and proximity of the sensor with respect to wall C. Based on the time of travel for the shock, the first pressure pulse at 2 ms is directly incident from the charge, followed shortly by three pressure pulses, two from wall C and one from combined reflection from the test cell floor and ceiling. This results in an initial peak in the cumulative impulse at 4 ms of 300 kPa ms as shown in Fig. 8b, which is 50 % higher than the impulse over the equivalent period in A1. There is then a clear negative phase in the pressure history between 4 and 6.5 ms, which is more significant than the equivalent negative phase seen in A1, which is thought to be caused by diffraction effects from the edge of the baffle. Between 7 and 16 ms there is very transient behaviour, with a significant number of smaller pressure peaks. The trend over this period is generally consistent, and although not all arrival times and magnitudes are the same for each shot, the cumulative impulse over this period shows good agreement between shots, with peak cumulative impulse values for all three shots between 470 and 510 kPa ms at 17 ms.

3.3 A3 results

Pressure time history from wall A in A3, shown in Fig. 9a, shows similar behaviour to that seen at the same location

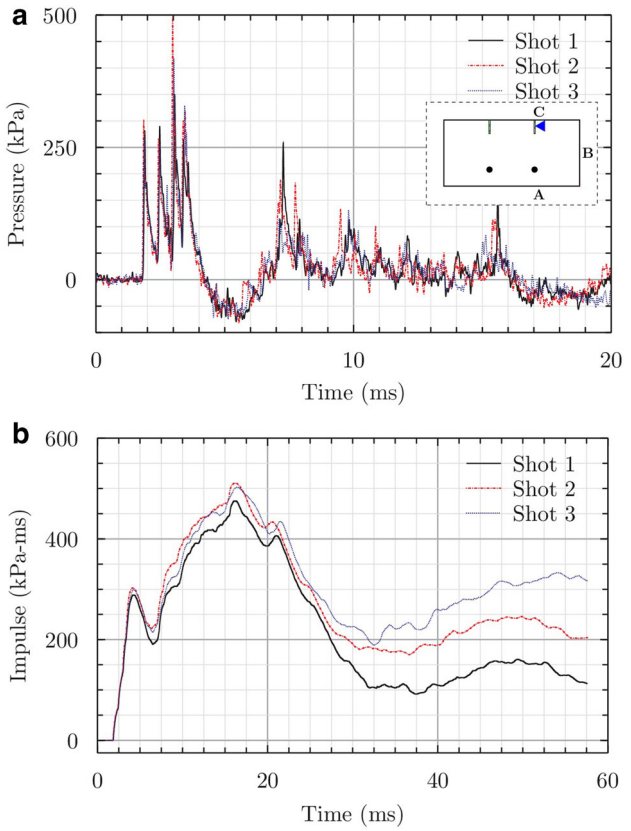

Fig. 8 Data from arrangement 2, location 2

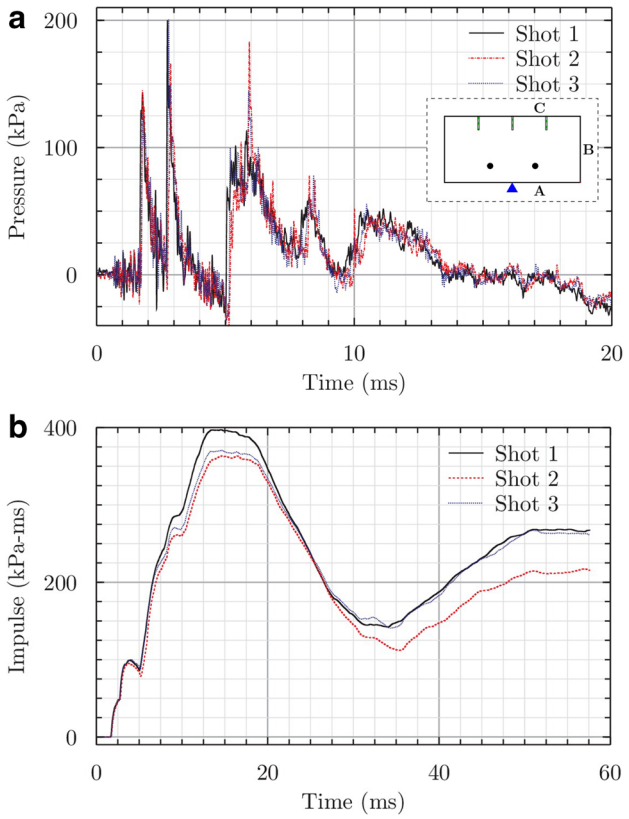

Fig. 9 Data from arrangement 3, location 1

for arrangement A2. The peak pressures (representing shock 1 and shock 2) are slightly lower than that seen in A2, but show a similar trend, with a 50–100 kPa difference between the first and second peaks displayed in both A1 and A2. The third peak occurs at a similar time to that seen in A2, but the decay is delayed in a similar fashion to that seen at the same point in A1. The fourth pulse in A3 is also significantly smaller than the equivalent shock in A2. Despite some clear differences between pressure histories, the impulse history is very similar to those in tests A1 and A2, with peak impulses for both between 370 and 400 kPa ms.

Figure 10a shows the pressure time history from the central baffle in A3 and shows a pattern of reflection similar to that seen at the baffle in A2. The first pressure peak in A3 arrives at 2.5 ms, slightly later than for the same shock in A2, due to the difference in distance from the charge. The following three peaks are separated by 0.5 ms, with magnitudes similar to A2, except the third shock which is around 100 kPa higher for all three shots.

The pressure between 7 and 16 ms again shows a number of reflections, but a quasi-static pressure of around 50 kPa between 7 and 10 ms, along with a period of increased positive pressure between 13 and 14 ms, means that the cumulative impulse at this location between 7 and 16 ms, shown in Fig. 10b, is slightly higher than that seen in A2, despite the sensor location being further away from the point of detonation.

It is worthwhile noting here that the pressure sensor data in Fig. 10a shows exceptional similarity between shots. It is often noted that there is a large degree of inherent variability in tests using high explosives, but experimental curves such as these demonstrate that careful test preparation and appropriate measurement tools enable capture of data which shows minimal variability between repeated tests. Although magnitudes of peak pressures cannot always easily be captured, due to their extremely high-frequency behaviour, the experiments show that the decay behaviour, shock timing and cumulative impulse can be captured with high levels of repeatability.

4 Discussion of results

4.1 Comparison with empirical data

The ConWep tool[1] is widely used to identify the pertinent parameters for free air and normally reflected explosions,

[1] The ConWep tool (Hyde [14]) is used to perform conventional weapons effect calculations and includes routines to calculate the free air blast parameters for bare explosives, such as peak pressure, arrival time and impulse.

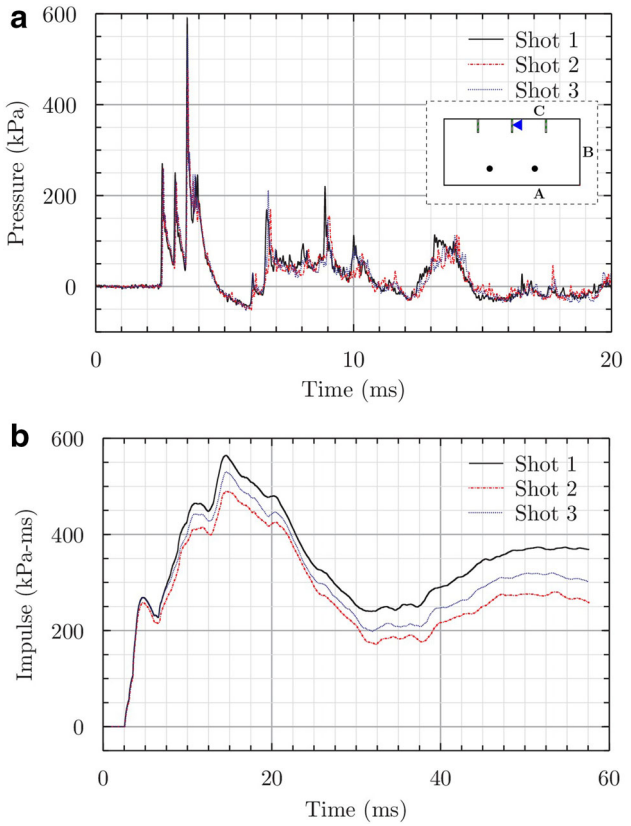

Fig. 10 Data from arrangement 3, location 2

and when used appropriately is accurate in a large number of circumstances. Comparisons of empirical data and the experimental data presented here can only be limited because this is not a simple free air explosion, but can offer insights into how realistic the assumption of symmetry at a rigid wall is.

As mentioned previously, the pressures measured at wall A are assumed to be the same as those that would be measured in free air for a test cell four times the width size, with a charge four times the size. Accordingly, the parameters measured for the first shock in location 1 in all arrangements should correspond to the ConWep side-on overpressure predicted at 1490 mm (the distance from charge to location 1; see Fig. 1) with a charge equivalent to 320 g of PE4. For a PE4:TNT mass equivalence of 1.2, giving a TNT input mass of 384 g, ConWep predicts results shown alongside parameters representing the experimental data[2] in Table 1.

Comparison between experimental data and ConWep shows good general agreement, but ConWep peak side-on overpressure is higher than that measured experimentally. For the highest experimental values, the difference compared to ConWep is small, but it is significant for the lowest measured peak pressure. The calculation of the pressure history in Table 1 is done by taking the impulse up until the point the following shock arrives, at which point the pressure has not reached zero (atmospheric)—in reality, some extra impulse would be added as the pressure continues to decay to zero, and as a result the method used to calculate the impulse here will underpredict the side-on pressure compared to ConWep.

[2] Some experimental parameters, notably the positive phase duration and cumulative impulse, can only be estimated, as the pressure is above zero when a second (reflected) shock arrives.

Table 1 ConWep predictions for 320 g PE4 at 1490 mm

	P_{so} (kPa)	t_a (ms)	t_d (ms)	i_{so} (kPa ms)
ConWep	184	1.5	1.5	65.5
Experiment	130–170	1.6	1.4[a]	50.0[b]

[a] Value estimated by extending curve down to meet the time axis
[b] Value cannot realistically be estimated, so value of cumulative impulse at arrival of next shock used

There are a number of reasons for the experimental peak pressure being lower than the ConWep prediction. First, despite efforts to ensure the area at the hinge operates as a symmetry plane, with all energy being directed out into the test cell, the inevitable destruction of the sacrificial stand-off packing means some energy is lost in the recess where the packing existed. Second, skin friction along test cell wall A will lead to an element of pressure loss, and will also somewhat slow down the shock, leading to the slightly later arrival time seen as pressure peaks in the experimental data. Finally, as the walls are not perfectly rigid, some energy will inevitably be lost to them due to elastic vibration. It is thought that in combination, these factors underlie the difference in peak pressure and hence cumulative impulse. However, calculation of experimental impulse values here were complicated by the presence of multiple shocks which limits straightforward comparison with ConWep data. Comparisons can only be made with measured side-on or normally reflected pressure predictions from ConWep, and only up until the time that the first reflected shocks arrive from other boundaries. In this work, it was assumed that location 1 measures the side-on overpressure up until a reflected shock arrived, between 2.5 and 2.8 ms.

4.2 Influence of rigid baffles

The presence of rigid baffles leads to an increase in peak cumulative impulse on wall A compared to the test case without baffles, as shown in Fig. 11. The increase primarily takes place between 6 and 12 ms, where an extra shock and extended region of high pressure after 10 ms are experienced in test arrangements A2 and A3, compared with A1. From Fig. 11 it can be seen that although the presence of baffles makes a change to the cumulative impulse, the change in number and spacing applied makes little difference. An extra shock is experienced at wall A as a result of reflections from the baffles, in addition to the reflections from wall C itself.

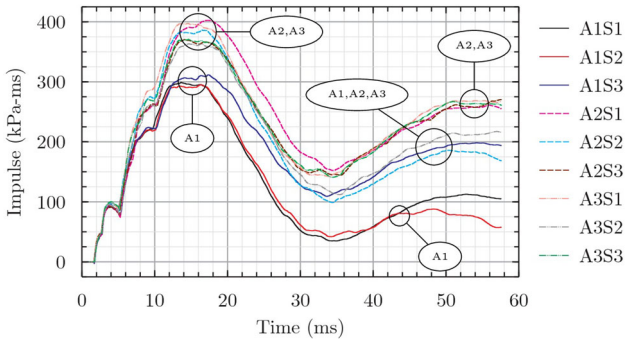

Fig. 11 Cumulative impulse history for all nine shots over the three test arrangements

At the points pressure was measured, there is also little evidence of significant attenuation of shocks by the presence of other baffles, either on wall C or wall A. It should be noted that the pressure peak from a shock seen at ∼7.5 ms in A2 and at ∼8 ms in A3 is different between the two arrangements, with a later arrival and noticeably lower magnitude in A3. This is likely to be a reflection from the baffle furthest from the charge, and the increased distance between the charge and baffle 3 in A3 compared to the charge and baffle 2 in A2 is probably responsible for the later arrival and lower magnitude. No measurements were taken behind the baffles, but the high levels of reflected shock experienced on the baffles, coupled with the angle they make with the incident wave, are likely to reflect shocks back towards an area that would otherwise have been shielded from the blast. The combination of reflection angles from different surfaces can be crucial in determining the peak pressures as shown by the higher magnitude of shock 3 in A3 compared to A2. However, the effect this has on the cumulative impulse at a point is generally limited due to the short duration of the shock. The cumulative impulse in this case is more dependent on lower magnitude, but longer duration pressure evolution.

4.3 Quarter symmetry testing

Quarter symmetry tests presented here offer an advantage both in terms of the size of experimental test facility required, especially when scaling is applied, and in terms of the mass of charge required. Had the experiments been carried out using twice the scale and without symmetry, a charge of 2.56 kg would have been required, as opposed to the 80 g used here (quarter symmetry gives a factor of 4, and scaling the radius by 2 gives a factor 2 cubed: 80 g × 4 × 8 = 2.56 kg). The data collected show that repeatable results can be achieved with this test configuration, with good shot to shot consistency seen in each test arrangement. Some divergence is seen in cumulative impulse results, but this is to be expected as the cumulative impulse is sensitive to slight positive or negative shifts in measured pressures; a shift of just 5 kPa between two data series over 50 ms will lead to a difference of 250 kPa ms at the end of this period, so the similarity seen in the cumulative impulse curves, which is generally within 50 kPa ms at peak cumulative impulse, shows that the test method is robust. The precise moulding of the charge and consistent fixed placement offer advantages over hand-rolled and hanging charges (which can be susceptible to movement), especially at smaller scaled distances where differences in the wave shape and standoff may be significant.

Improvements can be made both at the detonation point and along wall A (in wall roughness and exact symmetry of the charge energy distribution), to bring the experimental measurements more into line with the free air predictions from ConWep, although reasonable agreement was found between the ConWep side-on overpressures, arrival times and durations, and specific impulse up to the end of decay of the first shock wave.

5 Conclusions and further work

Quarter symmetry tests were undertaken, using a test configuration which has not previously been widely reported. This allows the size and number of resources required to carry out tests to be significantly reduced. While the results show that the assumption of symmetry is good, it is recognised that elastic deformation, surface roughness and other secondary issues mean that the walls do not in reality offer perfect symmetry, in the way that symmetry can do when employed in modelling. The test method was shown to be reliable and produced impressive shot to shot continuity. Further test work using the same test method is planned, to investigate the effect of structural deformation on confined blast pressures. Further work investigating the effect of baffles, their size, spacing and number would benefit from additional measurement locations, to give more detailed information about the effect of baffles on shock reflection phenomena.

Features similar to the baffles used in the tests presented here have been successfully demonstrated for blast attenuation in long structures such as tunnels. However, the experiments presented here show that when measurements are made closer to the charge attenuation is not seen. The peak pressures along the centre of the structure (i.e., the line of symmetry) are neither reduced nor increased, but the number of shocks experienced and the peak cumulative impulse are both increased. At the walls where the baffles are placed, interaction of multiple reflected shocks leads to both higher peak pressures and higher peak cumulative impulses com-

pared with when no baffles are present. The number and spacing of baffles was shown to have a limited effect on the pressures measured on the symmetry plane, wall A, of the test cell.

Acknowledgments The authors would like to thank the technical staff from the University of Sheffield and Blastech Ltd., particularly Jonny Reay, for test cell instrumentation and preparation, and the Advanced Additive Manufacturing group at the University of Sheffield for help with producing the charge mould. The authors are grateful for the Engineering and Physical Sciences Research Council (EPSRC) Doctoral Training Grant and to the Departments of Mechanical Engineering, and Civil and Structural Engineering at the University of Sheffield for funding this research. The authors are also grateful to the reviewers who provided constructive feedback during the preparation of this paper.

References

1. Anthistle, T.: Modelling the Effects of Blast Loads in Rail Vehicles. University of Sheffield (2014)
2. Rigas, F., Sklavounos, S.: Experimentally validated 3-D simulation of shock waves generated by dense explosives in confined complex geometries. J. Hazard. Mater. **121**(1), 23–30 (2005)
3. Smith, P.D., Vismeg, P., Teo, L.C., Tingey, L.: Blast wave transmission along rough-walled tunnels. Int. J. Impact Eng. **21**(6), 419–432 (1998)
4. Skjeltorp, A.T.: Airblast propagation through tunnels and the effects of wall roughness. In: DTIC Document (1975)
5. Neuscamman, S., Pezzola, G., Alves, S., Glenn, L., Glascoe, L.: Incorporating Afterburn Effects into a Fast-Running Tool for Modeling Explosives in Tunnels. Lawrence Livermore National Laboratory (LLNL), Livermore (2012)
6. Pope, D.: Design of a full-scale experimental blast tunnel. Proc. ICE Eng. Comput. Mech. **166**(3), 149–159 (2013)
7. Smith, P.D., Mays, G.C., Rose, T.A., Teo, K.G., Roberts, B.J.: Small scale models of complex geometry for blast overpressure assessment. Int. J. Impact Eng. **12**(3), 345–360 (1992)
8. Sauvan, P.E., Sochet, I., Trelat, S.: Analysis of reflected blast wave pressure profiles in a confined room. Shock Waves 1–12 (2012)
9. Togashi, F., Baum, J.D., Mestreau, E., Lohner, R., Sunshine, D.: Numerical simulation of long-duration blast wave evolution in confined facilities. Shock Waves **20**(5), 409–424 (2010)
10. Keenan, W.A., Tancreto, J.E.: Blast environment from fully and partially vented explosions in cubicles. In: DTIC Document (1975)
11. Chengqing, W., Lukaszewicz, M., Schebella, K., Antanovskii, L.: Experimental and numerical investigation of confined explosion in a blast chamber. J. Loss Prev. Process Ind. **26**(4), 737–750 (2013)
12. Edri, I., Savir, Z., Feldgun, V.R., Karinski, Y.S., Yankelevsky, D.Z.: On blast pressure analysis due to a partially confined explosion: I. Experimental studies. Int. J. Protect. Struct. **2**(1), 1–20 (2011)
13. Courant, R., Friedrichs, K.O.: Supersonic Flow and Shock Waves, vol. 21. Springer, New York (1976)
14. Hyde, D.W.: ConWep, conventional weapons effects program. US Army Engineer Waterways Experiment Station, USA (1991)